GKSS
FORSCHUNGSZENTRUM
in der HELMHOLTZ-GEMEINSCHAFT

Is the winter European climate of the last 500 years conditioned by the variability of solar irradiance and volcanism?

Authors:

P. Lionello
S. de Zolt
J. Luterbacher
E. Zorita

GKSS 2005/10

ISSN 0344-9629

GKSS 2005/10

Is the winter European climate of the last 500 years conditioned by the variability of solar irradiance and volcanism?

Authors:

P. Lionello

(University of Lecce, Italy)

S. de Zolt

(University of Padua, Italy)

J. Luterbacher

(University of Bern, Switzerland)

E. Zorita

(Institute for Coastal Research, GKSS Research Centre, Geesthacht, Germany)

GKSS-Forschungszentrum Geesthacht GmbH • Geesthacht • 2005

Die Berichte der GKSS werden kostenlos abgegeben.
The delivery of the GKSS reports is free of charge.

Anforderungen/Requests:

GKSS-Forschungszentrum Geesthacht GmbH
Bibliothek/Library
Postfach 11 60
D-21494 Geesthacht
Germany
Fax.: (49) 04152/871717

ISSN 0344-9629

GKSS-Forschungszentrum Geesthacht GmbH · Telefon (04152)87-0
Max-Planck-Straße 1 · D-21502 Geesthacht / Postfach 11 60 · D-21494 Geesthacht

GKSS 2005/10

Is the winter European climate of the last 500 years conditioned by the variability of solar irradiance and volcanism?

Piero Lionello, Simona de Zolt, Jürg Luterbacher, Eduardo Zorita

45 pages with 10 figures and 5 tables

Abstract

This study investigates the role of changes in solar irradiance and volcanism on the European winter climate during the past five centuries. The data are based i) on a 500-year long GCM simulation forced with reconstructions of solar and volcanic activity and concentrations of greenhouse gases and ii) on a chronicle-based reconstruction of the European temperature fields. The simulation shows multidecadal temperature variability that is correlated with the external forcing. The meridional temperature contrast (modeled and reconstructed) and precipitation (modeled) are associated with the North Atlantic Oscillation (NAO) at all time scales. At the multidecadal time-scale the simulated and empirically reconstructed mean European temperatures show common features during the Maunder Minimum (around 1700) and during the 20th century, in particular in northeastern Europe. However, also distinct discrepancies between the reconstruction and the simulation exist. In this respect temperatures over southern Europe are strongly correlated with the external forcing in the simulation but not in the reconstruction. Furthermore, the reconstruction shows a significant correlation between the external forcing and the NAO, which is not evident in the simulation.

Wurde das europäische Winterklima der letzten 500 Jahre durch Variationen der solaren Einstrahlung und des Vulkanismus bestimmt?

Zusammenfassung

In dieser Studie wird der Einfluss von Änderungen der solaren Einstrahlung und des Vulkanismus auf das europäische Winterklima der letzten fünfhundert Jahre untersucht. Die Datengrundlage bildet hierbei: i) eine 500 Jahre lange, mit Rekonstruktionen der solaren und vulkanischen Aktivität sowie Treibhausgaskonzentrationen angetriebene Simulation mit einem globalen Zirkulationsmodell, sowie ii): eine auf historischen Dokumenten basierende Rekonstruktion der europäischen Temperaturen. Die Simulation zeigt dekadische Temperaturvariationen, welche mit dem externen Antrieb korreliert sind. Der meridionale Temperaturgradient (im Modell und in der Rekonstruktion) steht auf allen Zeitskalen in Verbindung mit der Nordatlantischen Oszillation (NAO). Die simulierte und rekonstruierte mittlere Europatemperatur weisen Parallelen im Späten Maunder Minimum (ca. 1700) und im 20. Jahrhundert, insbesondere in Nordosteuropa, auf. Es bestehen allerdings auch deutliche Unterschiede zwischen Simulation und Rekonstruktion. In dieser Hinsicht sind die Temperaturen über Südeuropa mit dem externen Antrieb nur innerhalb der Simulation stark korreliert. Darüber hinaus zeigt die Rekonstruktion eine signifikante Korrelation zwischen dem äusseren Antrieb und der NAO, welche in der Simulation nicht vorhanden ist.

Manuscript received / Manuskripteingang in TDB: 10. November 2005

Contents

1 Introduction

This paper aims at evaluating the importance of the short-wave radiative forcing for the winter climate over Europe and to compare it to internal climate variability. This issue is relevant for regional climate studies and has important implications for the model capability to predict future climate scenarios at the regional scale. Europe is selected since it presents a well documented record of past climate variability, based on proxy-based reconstructions and the longest available instrumental time series (e.g. Luterbacher et al. 2004). The winter season is chosen because in wintertime the regional European temperature and precipitation fields are strongly connected to the NAO (North Atlantic Oscillation, e.g. Hurrell (1995), Hurrell and van Loon (1997), Hurrell et al. (2003), Jones et al. (2003) and, thus, it represents a situation where a large internal climate variability is present.

During the last 500 years, the Radiative Forcing (RF) of the Earth atmosphere has varied because of fluctuations of the solar radiation entering it and because of variations of its internal composition. The variations of solar radiation consist of decadal and multi-decadal fluctuations of solar irradiance (well-known periods of low solar activity are the Maunder Minimum, approximately from 1645 to 1715, and the Dalton Minimum, approximately from 1790 to 1820) and larger, abrupt, short-lived, reductions caused by volcanic eruptions, which sometimes occurred in sequences overlapping with minima of solar activity and further decreasing the available solar radiation. The effect of solar variability and volcanic eruptions can be merged into an effective total solar irradiance that represents the external short wave RF variability and will be referred to as SVRF (Solar and Volcanic RF) in this study. Besides this short wave contribution, the RF has varied also because of the increased long wave radiation associated to increased GHG (Green House Gases) concentration, largely due to human activities. The amount of observed European past climate variability that can be attributed to SVRF variability is still controversial, and, in this respect, the understanding of European regional climate dynamics in the last 500 years is incomplete.

Obviously, climate variability is caused, besides by the variations of RF, also by internal dynamics producing climate oscillations. In general these two effects are simultaneously present. The purpose of this study is to investigate the strength of the conditioning of the SVRF on the regional European climate, that is to distinguish the variability that is externally forced by changes of the incoming radiation from the internal variability of the climate system. This requires an analysis of the field behaviour at different timescales, as the effect of the SVRF is expected to be larger for longer timescales, and of the spatial distribution of correlation, as internal variability differentiates northern from southern Europe.

The study should also account for the possibility that part of internal variability could be influenced by the SVRF because of its possible effect on the main "natural" climatic oscillation modes affecting the European region. In other words, European temperature could be directly or indirectly forced by the time dependent RF. In this study a indirect forcing is discussed analysing the effect of the SVRF on the NAO phase or amplitude, being NAO the main climatic oscillation in this region.

The manuscript is organized in the following way. Sec.2 describes the data and tools used in this study. It consists of three subsections devoted to the description of the temperature reconstruction, NAO time series and model used in this study (sec.2.1, 2.2 and 2.3, respectively) in relation to other existing datasets and model simulations. Sec.3 describes the spatial distribution of correlation between the simulated European winter climate and both the SVRF and the NAO index, its dependence on the timescale, and the possible influence of the SVRF on the NAO time behaviour. Sec.4 analyses the reconstruction and compares it to the RF model simulation. Sec.5 discusses the results of this study and sec.6 presents its main conclusions.

2 Data used in this study

2.1 The reconstruction of European Temperature

The reconstructions of the European climate during the last millennium show the presence of large inter-annual and inter-decadal variability, and two main centennial oscillations, usually referred to as the MWP (Medieval Warm Period), from the 9^{th} to the 13^{th} century, with mild and warm characteristics, and the rather cold LIA (Little Ice Age), the downturn of temperature between 1350 and 1880, with totally three glacier advances in the Alps (around 1300-1380; 1570-1640; 1810-1850; Wanner et al. 2000). In fact, it is now recognized that were much more complex than the terms MWP and LIA imply, and the timing of the events varied regionally, if they can be discerned at all (Jones and Mann, 2004. Bradley et al 2003). The dramatic differences between regional and hemispheric past trends underscore the limited utility in the use of these terms. The period analysed in this study includes a large part of the LIA.

The present study uses a newly reconstructed gridded dataset (0.5 deg x 0.5 deg resolution), which includes European land-only temperature since 1500 (further referred to as "reconstruction" or Trc4), with seasonal resolution until 1658 and monthly afterwards (Luterbacher et al 2004). This spatial temperature reconstruction is based on a multi-proxy approach that includes homogenized early instrumental data series, calibrated documentary records[1] and natural proxy records[2], which provide all-year-round information about monthly or seasonal mean temperature fields, variability, spatial patterns of trends and of extremes. This in turn allows to assess quantitatively the degree of certainty and probability of the statements made and the conclusions drawn. The

[1]Documentary records are based on scientific writings, narratives, annals, monastery records, direction of cloud movement, wind direction, warm and cold spells, phenomenological information, freezing of water bodies, droughts and others which are interpreted by climate historians and translated to temperature values for different areas for Europe (Brázdil et al 1998)

[2]proxy records used in the reconstructions are tree ring data from Scandinavia and Siberia and ice cores from Greenland, which give indication about summer and winter temperature, respectively

methodology of Trc4 derived statistical models in order to get information on the relationships between the available data and the temperature distribution during the 20th century. These relationships were applied to the data in the period to be reconstructed in order to obtain the corresponding monthly or seasonal fields.

Fig.1 shows the average winter[3] European[4] temperature of the Trc4 reconstruction (black line). Time series have been obtained processing the original data with a digital low pass filter [5]. There is a short and intense cold period during the last decades of the 17^{th} century, approximately in correspondence with the Late Maunder minimum of solar activity and large volcanic eruptions, followed by a temperature increase during the first half of the 18^{th} century. This temporary recovery has been interrupted by a cooler period punctuated with a sequence of short cold spells, the last and largest of which took place at the end of the 19^{th} century. On the decadal scale, cold and warm episodes were characterized by temperature about 0.5K lower and higher than average, respectively. The following 20^{th} century record presents a warming trend, which shows appreciable differences with respect to the widely accepted global estimate of about 0.6K in 100 years (IPCC, 2001). Data show clearly that the period of most rapid warming in Europe occurred at the turning of the 20^{th}, between 1890 and 1910, and that there are large inter-decadal oscillations which hinder the identification of the two periods (from 1910 to 1945 and from 1976 onwards) characteristic of the warming trend at hemispheric scale. The latest warming period is not present in the plot because the filtered time series ends before its onset.

Reconstructions in general do not resolve intraseasonal variability and spatial distribution. Mann et al. (1998) published annual, boreal cold and warm seasonal spatial charts back to 1730, covering Europe. Fischer (2002) used a multi-proxy data set to reconstruct a summer temperature area-average for Europe back to 1761. Bradley and

[3]Winter consists of December, January, February

[4]The analysis carried out in this study considers the North-Atlantic and European Region (NAE), from 28.1^{o}W to 39.4^{o}E, and from 28.1^{o}N to 69.4^{o}N

[5]Filters with a 10, 20 and 40-year cut-off period have been used in this study.

Jones (1993) presented decadal averaged European temperature back to 1400 based on five regional proxy series. Guiot (1991) used a combination of documentary proxy evidence, European and Moroccan tree-ring data and δ^{18}O data from Greenland to provide annual temperature estimates from 1068-1979 for the area 35^oN-55^oN and 10^oW-20^oE. Using tree-ring data sets Briffa et al. (2001) reconstructed averaged northern and southern European growing season (April-September) temperature series back to the 17^{th} century. Additionally, Briffa et al. (2002) published maps of estimated April-September mean temperature for each year between 1600 and 1887 for parts of the North Hemisphere, including Europe. Some of these reconstruction were analysed by Hegerl et al. (2003), which reliably detected the response to volcanic forcing on the average northern hemisphere temperature, but found only a weak effect of solar variability, which is present only in some periods and some records. However, none of these reconstructions is adequate for the comparison with the monthly temperature regional distribution computed by the model.

2.2 NAO and its reconstruction

The NAO is a key climatic pattern for understanding the decadal variability of the European climate, as it is associated with a meridional contrast of temperature and precipitation (e.g. Hurrell (1995), Hurrell and van Loon (1997), Jones et al. (2003). The NAO is connected to the dominant signal of European precipitation and temperature, so that, over Northern Europe, its positive (negative) phases correspond to winters which are milder (colder) and wetter (drier) than average. Over Southern Europe, generally a positive (negative) winter NAO is associated with warmer (cooler) and drier (wetter) conditions over the northern part and cooler (warmer) and wetter (drier) over the southern part (Cullen and de Menocal, 2000; Xoplaki, 2002, Dünkeloh and Jacobeit, 2003; Xoplaki et al, 2004). The analysis of the connection between the NAO and the SVRF is an open issue and is basic for understanding the European climate variability and trends. Fig.1 (third row) shows the winter NAO index reconstruction for the last 500

years (denoted as Nrc2 in this paper), based on a combination of long instrumental series and documentary evidence (Luterbacher et al, 1999, Luterbacher et al. 2002). Other reconstructions of the winter NAO index are available (e.g Cook et al, 2002, shown in fig.1) and differences between them are important. For examples, the two reconstruction in fig.1 agree on the large negative peak during the Late Maunder minimum but differ considerably after it, when Cook et al. (2002) reconstruction[6] does not show the large positive peaks that are present in Luterbacher et al. (2002). Moreover, the persistent positive phase in the 19^{th} century is present only in Luterbacher et al. (2992). However, the correlation between the two reconstruction is statistically significant over the entire 500 years (tab.1). The differences among the various reconstructed NAO are extensively discussed elsewhere (Luterbacher et al. 2002; Cook et al. 2002, Schmutz et al. 2000, Timm et al. 2004). Differences between NAO reconstructions pose a limit on the confidence of the results that can be reached by this study as the errors that a single reconstruction contains can actually be larger than the signal.

2.3 The ECHO-G simulations

The model data used in this study have been produced using the ECHO-G model (Legutke and Voss 1999). The components of the model are atmospheric model ECHAM4 at T30 horizontal resolution (about 3.75× 3.75 degrees) [7] and the ocean model HOPE-G with a horizontal resolution of 2.8×2.8 degrees. The fields used for the analysis are SLP (Sea Level Pressure), T2 (Temperature at 2 meter level), P (Precipitation). The model reproduces satisfactorily the NAO and its link to the winter European temperature and precipitation patterns (Zorita and González-Rouco, 2002). At the same time, the stratosphere is only coarsely represented in the ECHAM4 model, which has only the four or five (depending on latitude) uppermost level inside it, the highest being 10hPa. This is admittedly a weak point, but a well resolved stratosphere would make the computer

[6]Note that Nrc2 considers Dec-Jan-Feb until 1658, while the Cook et al. (2002) includes also March.

[7]This resolution is only slightly lower that than often used in scenario simulations, typically T42

cost of a integration prohibitive. In fact, models with a more realistic stratosphere (as the model used by Shindell et al 2001b) have a much coarser horizontal resolution. The choice adopted by ECHO-G is the consequence of a necessary trade-off.

Two model simulations, denoted as RF and CTR (ConTRol) in this manuscript, have been carried out. In the 500-year long RF simulation a time dependent external RF was prescribed, that includes both the SVRF and the GHG contribution, that is the effects of variable solar activity, volcanic eruptions and increasing GHG concentration for the period from 1470 to 1990 (Fischer-Bruns et al 2002, Zorita et al 2004). The forcing due to volcanism is independent from the actual location of the eruptions and it is kept constant for the whole year, independently from the actual date of the events. In the 1000-year long CTR simulation a fixed annual cycle of RF corresponding to the 1990 level was prescribed.

The RF variability adopted in the model considers the 3 3 contributions mentioned in sec.1: fluctuations of solar irradiance, the effect of volcanic eruptions, and variation of GHG concentrations. Only the contribution of volcanic eruptions to the short-wave RF are considered in this study. Volcanic eruptions also contribute to changes in the long-wave forcing, but due to the difficulty of representing the physics of volcanic aerosols this forcing is also included in the effective solar constant. Fig.1, bottom panel, shows the external SVRF forcing represented by the effective total solar irradiance including the effect solar variability and volcanism. It was derived from the reconstructions of net radiative forcing provided by Crowley (2000) using his ^{10}Be/Lean splice. These reconstructions are essentially based on the ^{10}Be and sulphate aerosols records from ice cores, and on historical sun-spot observations. They involve conversions from concentration changes in ice cores to RF changes which are affected by uncertainty. The adopted scaling implies a change in the total solar irradiance (without considering the effect of volcanic aerosol) between the Late Maunder Minimum and today of about 0.35% , which is within the range (0.1-0.5%) suggested by IPCC (2001). Beside the Maunder Minimum (1645-1715), the SVRF (Radiative Forcing) was also characterized by the Dalton

Minimum (1790-1820), and by large volcanic eruptions. The third contribution is due to the GHG (Green House Gases) concentrations, derived also from concentrations in air bubbles trapped in ice cores. Anthropogenic aerosols have not been included in this analysis as they have been relatively important only in the last decades (IPCC, TAR 2001) whereas the focus of this study lies on the climate of the last centuries.

Many studies attempted to reproduce the present climate conditions and future scenarios, by considering both equilibrium and transient simulations, but the effort to model the observed climate variability of recent "historical" centuries has been limited. Cubasch et al. (1997) and Cubasch and Voss (2000) performed a transient simulation with variable solar radiative forcing since 1700 and found a clear signature of the RF on long term temperature variability. Further analysis were carried out by Hegerl et al. (1997). A detailed analysis including ensemble simulations, though limited to the 20^{th} century has been carried out by Tett et al. (1999, 2002). Crowley (2000) reproduced the hemispheric response to the single components (solar irradiance, volcanism, GHG) responsible for the RF changes with an Energy Balance Model. These studies conclude that the recent warming of the northern Hemisphere cannot be explained without resorting to the anthropogenic GHG increase. The analysis of the climate over Europe is more complicated, because of the larger variability present at several timescales and regional effects. Model simulations by Shindell et al (2001a) attributed the low European temperature in the Late Maunder minimum to an association between low solar irradiance and NAO negative phase. This would induce an amplification of a cold episodes over Europe, amplifying the cooling, otherwise modest on the hemispheric scale. Indeed, this mechanism as proposed by Shindell et al. (2001b, 2003) could also be responsible for the strong European winter warming and positive NAO trend for the late $17th$ century/beginning of $18th$ century reconstructed by Luterbacher et al. (2004). These results by Shindell et al. (2001b) rely on the inclusion of stratosphere dynamics in the model used, the NAO trend being much smaller if this component was not included in the model. At the same time the model used by Shindell et al. (2001b) uses a lower horizontal resolution (8 by

10 degrees) than the ECHO-G model used in this study and has no dynamical ocean so that their conclusions should be confirmed by higher resolution and more comprehensive coupled models.

3 Relation between NAO index, Radiative Forcing and European climate in the ECHOG-simulations

The spatial distribution of the correlation between the winter T2 and P fields and the NAO index in the ECHO-G simulations over the NAE (North Atlantic and European) region has been computed. The NAO index is given by the mean value of the normalized SLP difference between Azores and Iceland. Results are shown in fig.2 and 3, left (CTR) and central (RF) columns. The correlation of the T2 and P fields to the time dependent SVRF that was used in the RF simulation has been also computed (fig.2 and 3, right column). Besides considering the time series of average winter values (top row in fig 2 and 3) the correlation has been computed at 3 other different time scales by applying a digital low-pass (in frequency) filter with a 10year, 20year and 40year cut-off period[8] (second to fourth rows, respectively). The first 80 years of the RF simulation were taken as spin-up period and not included in the analysis.

The correlation of T2 and P fields with the NAO index has completely different characteristics than that with the SVRF. The correlation with the NAO index presents a weaker dependence on timescale, conserving the same basic structure for the yearly and the filtered data. It shows the characteristic dipole, corresponding to the advection of warm humid air towards northern Europe during the positive NAO phase, and towards Southern Europe during the negative phase, which agrees with the well-known observed distributions and indicates that the ECHO-G simulation reproduces correctly the link of the European climate to NAO. On the contrary, the correlation of T2 with the SVRF

[8]The degrees of freedom of the filtered time series, which are reduced as the cut-off period increases, have been estimated as N_{year}/N_F, where N_F has been estimated by applying the filter to a white noise time series and taking the time interval required for the autocorrelation to vanish. It resulted $N_F = 6, 16, 25$ for the 10, 20, 40-year cut-off, respectively. This has been accounted for in the analysis.

increases with the length of the timescale, becoming larger than that with NAO at long timescales. It has a zonal distribution with the largest values at the southern coast of the Mediterranean Sea. Correlation of P with SVRF is negligible over most continental Europe, but in the 40-year low-pass filtered time series, where higher SVRF is linked to an increase of precipitation over the North and the Norwegian Seas, and to a reduction over the mid latitude Atlantic.

A more detailed analysis of the spatial correlation of the T2 and P with the NAO shows a small, but interesting, different characteristic in the CTR and RF simulations. While the patterns based on average winter values are very similar, those based on 40-year low-pass filtered data are appreciably different. In the CTR simulation, for increasing timescales, the northern positive lobe in the correlation map of T2 with NAO occupies an increasingly large area and the negative lobe of the correlation with P moves north-eastward to Southern Europe. In the RF simulation, the northern positive lobe in the correlation map of T2 moves eastward and the southern negative one moves northward inside the Mediterranean Sea. In the correlation map with P, the features above Scandinavia and Southern Central Europe become stronger for increasing timescales. This behaviour corresponds to the different timescale dependence of the SLP variability over the Atlantic, as shown in Fig.4, where the first EOF of the winter SLP fields, that is the NAO dipole, is plotted at different timescales. At the inter-annual timescale the CTR and RF simulations are very similar, but, for increasing timescales, the axis of the dipole has a small anticlockwise rotation in the CTR simulation and a clockwise rotation in the RF simulation. Consequently, with longer timescales, the European climate is more strongly associated with the variability of the advection of air masses from sub-tropical Atlantic in the CTR simulation and of those from North Atlantic in the RF simulation. This behaviour may indicate an effect, though weak, of the SVRF on the structure of NAO.

Four indices[9] have been computed in order to summarize the characteristics of the

[9]Indices of both RF and CTR simulations have been computed subtracting the average value and

behaviour of the T2 and P fields (fig.6). The mean temperature and the total precipitation indices represent the variability of the average value of T2 and P over the whole area. The temperature and precipitation contrast indices (denoted with ΔT2 and ΔP) have been computed as the difference between average values over two selected areas (fig.5), representative of northern and southern Europe. The selected areas are different for the precipitation and the temperature contrast index. Positive values of the contrast index correspond to positive anomalies over Southern Europe and negative anomalies over northern Europe. These two indices represent the strength of the dipole affecting the spatial distribution of T2 and P. Time series of the indices are shown in fig.6. The difference between the two simulations is very clear for the T2 index, which in the RF simulation presents a much higher variability and two very cold periods in correspondence to the Late Maunder and Dalton minima of solar activity (two periods characterized also by strong and frequent volcanic eruptions), and a positive trend since the last part of the 19^{th} century. The corresponding T2 index of the CTR simulation presents a smaller variability, and a higher average level, which is consistent with the constant 1990 RF forcing set for the whole CTR simulation.

Results are summarized in tabs.2 and 3. The NAO correlation with ΔT2 and ΔP is very large, it is practically constant over the different timescales, and has similar values in the RF and CTR simulation, varying in the interval from 0.6 to 0.75. The sign of the correlation of NAO with the average values over the whole area of T2 and P reflects the dominant role of the positive correlation over northern Europe for T2 and of the negative correlation over southern Europe for P. In the CTR simulation, the dependence of the spatial distribution of the correlation with the timescale results in an increasing/decreasing correlation of NAO with the average value of T2/P over the NAE region. The opposite dependence is present in the RF simulation. The SVRF is clearly, and somehow obviously, very well correlated with the average European temperature for

normalizing with the variance of the last 500 years of the CTR simulation. This was, obviously not possible for the SVRF index, which has been computed using the values of the RF simulation itself.

long timescales, but has no significant link to the other indices.

Therefore, the NAO is correlated with the contrast of the T2 and P fields between North and South Europe at both inter-annual and decadal timescales. The NAO correlation with the average European T2 and P has a timescale dependence which reveals an effect of the SVRF at the multi-decadal timescales. The importance of the SVRF for the European temperature field at multi-decadal timescales is comparable to or larger than that of the NAO, while at shorter timescale the influence of NAO is much larger.

Though, sometimes, a visual association between minima of SVRF and NAO index can be identified in fig. 1, no statistically significant correlation has been found between the NAO index and the SVRF (tab.3). Apparently, no linear relation between SVRF and NAO is present in the RF simulation, though perhaps a non-linear effect cannot be completely ruled out.

Other effects of the SVRF on the NAO have been considered, but with inconclusive results. One explored possibility is the presence of recurrent disruptions or perturbations of the NAO patterns. Fig.7 shows the first EOFs of the (unfiltered) winter mean SLP fields over the Atlantic in some periods corresponding to very large negative decadal oscillations of the NAO index. These periods correspond to the Late Maunder and Dalton periods of solar activity in the RF simulation, and two periods, from 650 to 700 and from 400 to 450, in the CTR simulation. Results show only minor variations. It is important to observe that large fluctuations of the NAO index and are not present in the RF simulation only. Actually, the most remarkably persistent negative NAO condition, with an almost 50-year long duration, is present in the CTR simulation between year 400 and 450 and it has already been noted to present climate anomalies (Zorita et al., 2003). This period does not seem, however, to result in a deformed NAO dipole.

Fig.8 (left panel) shows the statistical distribution of the winter NAO index in the instrumental data (Jones et al. 1997), and in the RF and CTR simulation. Though the RF and CTR distributions appear similar, the RF simulation presents an improvement in reproducing the skewness of the observed distribution. Comparison of spectra (Fig.8,

right panel) leads to controversial conclusions. On the one hand the differences between RF and CTR are statistically significant and the RF spectrum reproduces the observed 6 year peak. This would suggest an effect of the SVRF on the NAO spectrum. On the other hand the NAO simulated in the RF simulation presents a large unrealistic gap in the 8 year band, which has, instead, approximately the right level in the CTR simulation. Note that the differences between RF and CTR spectra do not match the peaks in the RF spectra (not shown), so that the eventual link is weak and nonlinear. Moreover, this analysis suggests that the model simulations might not be capable of fully reproducing the correct energy distribution of the observed NAO.

Tabs.4 and 5 compare the mean value and the variance of the Azores-Iceland winter monthly SLP difference in model simulations and instrumental observations (Jones 1987) selecting different time intervals. For the instrumental record the two parameters have been computed until 1990 (final year of the RF simulation) considering the last 25, 70, 125 years (this is the longest possible record). The period has been extended to 450 years for the RF simulation and also to 1000 years for the CTR simulation. No data set shows a significant trend if statistical uncertainty is taken into account. Considering the 125-year long period, the difference between RF and CTR simulations is statistically significant, with the CTR overestimating and the RF underestimating the instrumental mean value. This difference would be consistent with a positive correlation between RF and NAO, because the radiative forcing value in the CTR simulation (fixed at the 1990 level) is higher than in the RF simulation. In fact, during the last 25-year long period, when both simulations have a comparable RF, both simulated mean values are compatible with the instrumental one, though the RF simulation is much closer to it. The variance of NAO index is similar in the two simulations, and smaller than the the instrumental value. However, they cannot be considered statistically different, in view of the large confidence intervals of the estimates.

4 European climate reconstruction: the relation between NAO index, Radiative Forcing and winter temperature

The correlation between the reconstructed surface air temperature (fig.9) and the NAO from Nrc2 shows the well known dipole structure (the reconstruction of NAO of Luterbacher et al. (2002) has been used). In the reconstruction, the northern positive lobe is much wider, so that the correlation with the average European temperature is higher than in the simulations (tab.2). Moreover, the tendency of the correlation to decrease with longer timescale, though present, is not as large as in the RF simulation.

In Trc4, the correlation of average surface temperature with RF is small at all time scales (fig.9 and tab.3). This is a consequence of the negative correlation between SVRF and temperatures in northern Africa, which compensates the small positive correlation between SVRF and temperatures in the remaining parts of Europe. The average temperature, thus, is uncorrelated with SVRF. This North African negative correlation is certainly a puzzling feature, which may be artificially due to the lack of data in this region. In fact, the temperature reconstruction here is mostly based on its statistical link with temperature in Europe.

The dipolar structure of the correlation between SVRF and temperature might actually be due to the anti-correlation between reconstructed European and North African temperatures, this anti-correlation being caused by the influence of the NAO on both temperatures in the instrumental period. Therefore, if European temperatures are positively correlated with SVRF (a reasonable assumption), North African temperatures would artificially appear anti-correlated with SVRF.

Another aspect is that the reconstruction of the NAO index and of temperatures are not completely independent, as part of the proxy indicators are used in both reconstructions. This may explain the high correlation, increasing with the timescale, of the NAO and SVRF (tab.3). This trend is characteristic of the Nrc2 NAO reconstruction and it is

present neither in the RF simulation nor in the Cook et al. (2002) reconstruction. Actually the two NAO reconstructions show some agreement on inter-annual variability, but a correlation decreasing with time-scale, so that long period fluctuations of the NAO index in these two time series differ. A similar effect has been detected in analysis of NAO reconstructions with synthetic data from GCM simulations (Zorita and González-Rouco, 2002) (tab.1).

Fig. 1 shows the reconstructed (Trc4) and simulated (RF) average European land temperature time series filtered with a 10-year (top panel) and 40-year (second row) low pass filter. The RF simulation presents a much larger variability than the reconstructions. In spite of this, the correlation between simulated and reconstructed mean European temperature is significant and it increases with the timescale (tab.3). The two time series show a remarkable agreement during the cool period of the Maunder minimum and the subsequent warming. The opposite behaviour is seen in the southern part of the analysed region, where the correlation of the Trc4 temperature with the SVRF is negative and that of the RF simulations is large and positive. This hinders a satisfactory agreement between the respective average temperature time series.

In order to investigate the correlations at grid-point level between the RF and Trc4 fields, the latter have been "up-scaled" from their $0.5^o \times 0.5^o$ degrees resolution to the $3.75^o \times 3.75^o$ resolution of the gridded ECHO-G data, by taking the average value in each ECHO-G grid box. Boxes that resulted less than 50% filled with data have been ignored. Also the sea points of the ECHO-G simulation were not included, so that the analysis is based only on points that, at the $3.75^o \times 3.75^o$ resolution, can be considered land for both the reconstruction and the RF simulation. The correlation has been computed including data from the period 1550 to 1990. Results are shown in fig.10. Correlation is nowhere significant at the inter-annual timescale, but increases with timescales, becoming significantly large for multi-decadal timescales on north-eastern Europe, while it remains not significant on Southern Europe and on the northern African coast of the Mediterranean Sea. This pattern is consistent with the correlation between temperature and SVRF in

the simulation and in the reconstruction.

There are two reasons for the different behaviour over northern Africa, where both datasets are presumably not quite reliable. In the model simulation, the land-sea mask in the Mediterranean sea region is not accurate (see fig.5) and the Gibraltar Strait is replaced with a 1000 km wide sea extent. It would not be surprising that the characteristics of Mediterranean air mass are not properly reproduced in the simulation. Moreover, no temperature sensitive proxy data are available for the reconstruction over northern Africa before the end of the 19^{th} century, so that the features over this region results solely from their connection with European temperatures, which has been established mostly using instrumental data at inter-annual timescales. The NAO is expected to have a marginal role in the explanation of the correlation between simulated and reconstructed temperature, as the relative NAO time series are not correlated. At the same time the absence of correlation between simulated and reconstructed NAO is partially responsible for the lack of correlation between the simulated and reconstructed temperatures at inter-annual timescale.

5 Discussion

This study analysed the relative strength of the conditioning exerted by the NAO and by the RF on the regional European climate in the past few centuries. The analysis of the results has some importance also for future regional climate change , at least for future periods when the assumed RF changes do not grossly exceed past variations.

A key aspect is that the effect of the SVRF and the NAO may be entangled by the influence of SVRF on the NAO itself. This is an important issue, because the absence of correlation between NAO and SVRF would limit the possibility to reconstruct, or predict, a major component of the inter-annual and decadal variability of European Climate. However, the presence of a strong phase lock between SVRF and NAO is controversial. The Nrc2 reconstruction of the NAO index is the only time series which shows a significant correlation between the SVRF and the NAO at decadal and multi-decadal timescales, while the Cook et al. (2002) data and the RF model simulation

do not present a similar behaviour. Since other modelling studies suggest a stronger conditioning of the RF on the NAO if the stratospheric dynamics is well represented (Shindell et al 2001a, 2001b), the lack of correlation between NAO and SVRF might be explained by the coarse representation of the stratosphere in the ECHO-G model. On the other hand the link of NAO to SVRF could be nonlinear and present only in particular situations, like the Late Maunder minimum, at the end of which both reconstructions show a negative large NAO index, and also the RF simulation has a large negative values, though about 10 years earlier than the two reconstructions. However, accepting that validity of the Nrc2 NAO reconstruction, the link of SVRF to NAO would be practically relevant only at multi-decadal time scales.

In this study a series of possible effects of the SVRF on the NAO, have been considered with inconclusive results. The shape of the statistical distribution of the Azores-Iceland pressure seems closer to observations in the RF than in the CTR simulation. The statistics of this quantity show that the RF and CTR simulations have opposite errors for its mean value (the RF simulation underestimates it) and both underestimate its variance. Accounting for statistical errors both the RF and CTR simulations provide estimates that are consistent with instrumental observations. The consistency margin is very narrow for the Azores-Iceland pressure difference variance, suggesting that variability is underestimated in the model simulations. The difference of the mean value between the RF and CTR simulations is statistically significant suggesting that high SVRF values would increase the meridional pressure gradient. The analysis of the NAO spectra does not lead to clear conclusions. Finally, the evidence that the usual NAO pattern has been partially distorted during the periods corresponding to large negative decadal oscillations of the NAO index are unconvincing, as large negative oscillations are present both in the RF and in the CTR simulation.

There is a remarkable aspect of the behaviour of the NAO at multi-decadal timescales. In the RF simulation the axis of the NAO dipole rotates clockwise for increasing time scales. This diminishes the advection of humid and warm air over northern Europe

from mid-Atlantic, so that the positive lobe of the correlation relating the NAO index to the temperature and precipitation fields over northern Europe shrinks. This causes a decreasing correlation with timescale of the average European temperature and an increasing anti-correlation of the overall European precipitation with the NAO index. The reconstruction does not exclude this trend as correlation of its winter temperature with NAO decreases with the timescale.

RF simulation and reconstruction do not agree on the effect of SVRF on European Climate during the last five centuries. In the RF simulation, at the multi-decadal timescale, the SVRF conditioning of European climate becomes comparable to, or even larger than, that of NAO in the southern part of the analysed region. On the contrary, the reconstruction does not show a significant correlation, and it presents a negative correlation to SVRF above northern Africa. This may be caused by the observed anti-correlation between European and North African temperatures at interannual timescales, which leaves its imprint on the reconstructed North African temperatures.

In fact, northern Africa is a region where the SVRF conditioning should be strong and the lacking correspondence between reconstruction and RF simulation over this area is disappointing. Neither the RF simulation, nor the reconstruction appear in this situation very reliable. ECHO-G is characterized by very coarse model resolution and an unrealistic land-sea mask in the Mediterranean Region. The reconstruction is based on few local proxies and it is derived mostly by its statistical relation with the temperature over Europe.

It is clear that the results of this study are affected by large uncertainties and different datasets lead to different interpretations. Both reconstructions and simulations present shortcomings. Lack of agreement on long term fluctuations of NAO and on temperature are evident comparing different reconstructions. Differences between model simulations are justified by simplifications which the models are forced to adopt for integrations covering multi-centennial periods. It is difficult to establish a priori whether the results of some model are more reliable than others, that is if the simplified ocean and the lack

of resolution of the study by Shindell et al. (2001b) are more crucial than the coarse resolution of the stratosphere in ECHO-G. It is also not clear if the reconstructions tend to underestimate the temperature variability or the ECHO-G model is over-sensitive to the variations of the RF. Moreover, other effects not included in the model, as land use changes, can be also important (Bauer et al 2003). Finally, five centuries are a short period for multi-decadal variability and the availability of longer simulations could help to reduce uncertainties.

6 Conclusions

There are two conflicting interpretations of the results of this study, which appear difficult to reconcile. According to the RF simulation, NAO has no linear relation to the SVRF, so that predictability of temperature would be restricted to the part of the temperature variability directly determined by the RF alone. In future studies, a set of multi-model simulations could offer important information for confirming this interpretation. On the other hand, in the reconstruction there is a linear correlation between NAO and SVRF, which increases with the time scale, so that the predictability may be enhanced by the additional contribution of the NAO. However, other reconstructions of NAO do not agree on this multi-decadal behaviour, so that correlation between NAO and SVRF could be a peculiarity of the Nrc2 reconstruction.

In our view, the most likely interpretation of these results is that, at regional scale, the SVRF conditioning of temperature becomes dominant only at multi-decadal timescales as shown by the RF simulation, and shorter timescales are dominated by intrinsic climate variability, which could be chaotic and unpredictable. It remains possible that the effect of SVRF on NAO is nonlinear and appears only in particular situations, such as the Maunder Minimum, while in general NAO is weakly linked to the SVRF. If confirmed, this would indicate that part of future European temperature changes will be associated with, internal, eventually unpredictable, climate dynamics. This conclusion should not be extrapolated to very general validity: other regions or other seasons less under the influence of internal variability would present a more predictable behaviour. Moreover,

in climate change scenarios, the variation of the RF forcing is much larger than that accounted for in this study, and the RF effect could be more dominant.

Acknowledgements P.Lionello thanks the GKSS Forschung Zentrum for the hospitality during his sabbatical year. S.De Zolt has been partially supported by the GKSS Forschungszentrum J. Luterbacher has been supported by the Swiss National Science Foundation (NCCR Climate) and by the EU project SO&P. E. Zorita's contribution was performed in the frame of the German program DEKLIM.

The CRU data were downloaded from the CRU (Climate Research Unit, Univ. of East Anglia) web page http://www.cru.uea.ac.uk. Cook et al. (2002) NAO time series has been extracted from data archived at the World Data Center for Paleoclimatology, Boulder, Colorado, USA (web page: http://www.ngdc.noaa.gov/paleo).

References

[1] Bauer, E, Claussen M, Brovkin V, . Huenerbein A (2003) Assessing climate forcings of the Earth system for the past millennium Geophys. Res. Lett. 30: 1276 DOI: 10.1029/2002GL016639.

[2] Bradley RS, Jones PD (1993) 'Little Ice Age' summer temperature variations: their nature and relevance to recent global warming trends. The Holocene 3: 367-376.

[3] Bradley RS, Hughes MK, Diaz HF (2003) Climate in Medieval Time. Science 302: 404-405.

[4] Brázdil, R., Pfister, C., Wanner, H., von Storch, H., and Luterbacher, J., (2004) Historical climatology in Europe The State of the Art, Clim. Change 70, 363-430.

[5] Briffa KR, Osborn TJ, Schweingruber FH Harris IC, Jones PD, Shiyatov SG Vaganov EA (2001) Low-frequency temperature variations from a northern tree-ring-density network. J. Geophys. Res. 106: 2929-2941.

[6] BriffaKR, Osborn TJ, Schweingruber FH, JonesPD, Shiyatov SG Vaganov EA (2002) Tree-ring width and density data around the Northern Hemisphere: Part 2, spatio-temporal variability and associated climate patterns. The Holocene 12:759-789.

[7] Cook ER, D'Arrigo RD, and Mann ME (2002) A Well-Verified, Multiproxy Reconstruction of the Winter North Atlantic Oscillation Index since A.D. 1400. Journal of Climate 15: 1754-1764.

[8] Crowley TJ (2000) causes of climate change over the past 1000 years. Science 289: 270-277.

[9] Cubasch U, Hegerl GC, Voss R, Waskewitz J Crowley TC, (1997) Simulation with an O-AGCM of the influence of variations of the solar constant on the global climate. Clim. Dyn. 13: 757-767.

[10] Cubasch U, Voss R (2000) The influence of total solar irradiance on climate. Space Science Reviews 94: 185-198.

[11] Cullen HM, de Menocal PB (2000) North Atlantic influence on Tigris-Euphrates streamflow. Int. J. Climatol. 20: 853-863.

[12] Dünkeloh A, Jacobeit J (2003) Circulation dynamics of Mediterranean precipitation variability 1948-1998. Int J Climatol 23: 1843-1866.

[13] Fischer DA (2002) High-resolution multiproxy climatic records from ice cores, tree-rings, corals and documentary sources using eigenvector techniques and maps: assessment of recovered signal and errors. The Holocene 12: 401-419.

[14] Fischer-Bruns I, Cubasch U, von Storch H, Zorita E, González-Rouco JF, Luterbacher J (2002) Modelling the Late Maunder Minimum with a 3-dimensional OAGCM, CLIVAR exchanges 7: 59-61.

[15] Guiot J. (1991) The combination of historical documents and biological data in the reconstruction of climate variations in space and time in Frenzel, B., Pfister, C., and Glaeser, B. (eds.), European Climate Reconstructed from Documentary Data: Methods and Results, Gustav Fischer Verlag, Stuttgart, Jena, New York, pp. 93-104.

[16] Hegerl GC, Hasselmann K, Cubasch U, Mitchell JFB, Roeckner E, Voss R, Waszkewitz J (1997) Multi-fingerprint detection and attribution analysis of greenhouse gas, greenhouse gas-plus-aerosol and solar forced climate change. Clim. Dyn. 13: 613-634.

[17] Hegerl G C, Crowley TJ, Baum SK, Kim K-Y, Hyde WT (2003) Detection of volcanic, solar and greenhouse gas signals in paleo-reconstructions of Northern Hemispheric temperature. Geophys,. Res. Lett 30(5): 12-42. doi: 10/1029/2002GL016635.

[18] Hurrell JW (1995) Decadal trends in the North Atlantic Oscillation and relationships to regional temperature and precipitation. Science 269: 676-679.

[19] Hurrell JM , van Loon H (1997) Decadal variations in climate associated with the North Atlantic Oscillation. Clim. Change 36: 301-326.

[20] Hurrell JW, Kushnir Y, Otterson G, Visbeck M(Eds.), (2003) North Atlantic Oscillation, Climatic Significance and Environmental Impact. Geophysical Monograph 134, American Geophysical Union (AGU), Washington.

[21] IPCC (2001) Climate change 2001: the scientific basis. Cambridge University Press, Cambridge, UK, 881pp.

[22] Jones PD (1987) The early twentieth century Arctic High - fact or fiction? Clim. Dyn. 1: 63-75.

[23] Jones PD, Jönsson T, Wheeler G (1997) Extension to the North Atlantic Oscillation using early instrumental pressure observations from Gibraltar and South-West Iceland. Int. J. Climatol. 17: 1433-1450.

[24] Jones PD , Osborn TJ, Briffa KR (2003) in The North Atlantic Oscillation: Climatic Significance and Environmental Impact [Geophysical Monograph 134], J. W. Hurrell, Y. Kushnir, G. Ottersen, M. Visbeck, Eds. (American Geophysical Union, Washington, DC.

[25] Jones PD, Mann ME (2004) Climate Over Past Millennia. Rev. Geophys., 42: RG2002, doi: 10.1029/2003RG000143.

[26] Legutke S , Voss R (1999) ECHO-G, The Hamburg Atmosphere-Ocean Coupled Circulation Model , DKRZ-Report n.18, 43pp.

[27] Luterbacher J, Schmutz C, Gyalistras D, Xoplaki E, Wanner H (1999) Reconstruction of monthly NAO and EU indices back to AD 1675, Geophys. Res. Lett. 26: 2745-2748.

[28] Luterbacher J, Xoplaki E, Dietrich D, Jones PD, , Davies TD, Portis D, González-Rouco JF, von Storch H, Gyalistras D, Casty C, and Wanner H (2002) Extending North Atlantic Oscillation Reconstructions Back to 1500. Atmos. Sci. Lett. 2:114-124 doi:10.1006/asle.2001.0044.

[29] Luterbacher J, Dietrich D, Xoplaki E, Grosjean M, WannerH (2004) European seasonal and annual temperature variability, trends, and extremes since 1500. Science 303: 1499-1503 (DOI:10.1126/science.1093877).

[30] Mann ME, Bradley RS, Hughes MK (1998) Global-Scale Temperature Patterns and Climate Forcing Over the Past Six Centuries Nature 392: 779-787.

[31] Mann, ME, Gille E, Bradley RS, Hughes MK, Overpeck JT, Keimig FT, and W. Gross, (2000) Global Temperature Patterns in Past Centuries: An interactive presentation, Earth Interactions, 4-4, 1-29.

[32] Shindell DT, Schmidt GA, Mann ME, Rind D, Waple A (2001a) Solar forcing of regional climate change during the Maunder Minimum. Science 294: 2149-2152.

[33] Shindell DT, SchmidtGA, Miller RL, Rind D (2001b) Northern Hemisphere winter climate response to greenhouse gas, ozone, solar, and volcanic forcing. J. Geophys. Res. 106: 7193-7210.

[34] Schmutz C, Luterbacher J, Gyalistras D, Xoplaki E, Wanner H. (2000) Can we trust proxy-based NAO index reconstructions? . Geophys. Res. Lett. 27: 1135-1138.

[35] Stine S (1998) Medieval Climate Anomaly in the Americas. In: Water, Environment and Society in Times of Climatic Change (eds. A.S. Issar und N. Brown). Kluwer, Dordrecht, 43-67.

[36] Tett SFB, Stott PA, Allen MA, Ingram WJ , Mitchell JFB (1999) Causes of twentieth century temperature change. Nature 399: 569-572.

[37] Tett SFB Jones GS, Stott PA, Hill DC , Mitchell JFB , Allen RM , Ingram WJ , Johns TC, Johnson CE, Jones A, Roberts DL, Sexton DM , Woodage MJ (2002) Estimation of natural and anthropogenic contributions to twentieth century temperature change. J. Geophys. Res. 107: 4307 .

[38] Xoplaki E, González-Rouco JF , Luterbacher J , Wanner H, (2004) Wet season Mediterranean precipitation variability: influence of large-scale dynamics, Clim. Dyn. 23: 63-78, (DOI 10.1007/s00382-004-0422-0).

[39] Xoplaki E (2002) Climate variability over the Mediterranean. PhD thesis, University of Bern, Switzerland . ([http://sinus.unibe.ch/klimet/docs/phd_xoplaki.pdf])

[40] Zorita E , González-Rouco JF (2002) Are temperature proxies adequate for North Atlantic Oscillation reconstructions ? Geophys. Res. Lett. 29: 102019, 48-1-48-4.

[41] Zorita E, González-Rouco JF, Legutke S (2003): testing the Mann et al (1998) approach to paleoclimate reconstruction in the context of a 1000-yr control simulation with the ECHO-G Coupled Climate model, J Climate 16:1378-1390.

[42] Zorita E, von Storch H, González-Rouco JF, Cubasch U, Luterbacher J , Fischer-Bruns I, Legutke S , Schlese U (2004) Climate evolution in the last five centuries simulated by an atmosphere-ocean model: global temperatures, the North Atlantic Oscillation and the Late Maunder Minimum, Meteorol. Zeitschrift 13: 271-289.

Correlation: NAO

	1-winter	10 y	20 y	40 y
Nrc2 $<->$ Cook	**0.41**	**0.34**	(0.31)	(0.17)

Correlation: T2

Trc4 $<->$ RF	(0.01)	**0.26**	**0.40**	**0.48**

Table 1: Top row: correlation between the NAO index Nrc2 of Luterbacher et al. (2002) and that of Cook et al. (2002). Bottom row: correlation between the average European winter temperature Trc4 of Luterbacher et al. (2004) and that of the RF simulation.

Correlation with NAO index

	1-winter	10 y	20 y	40 y
T2 (RF)	**0.21**	**0.27**	(0.26)	(0.12)
ΔT2 (RF)	**-0.60**	**-0.64**	**-0.72**	**-0.74**
P (RF)	**-0.37**	**-0.34**	**-0.38**	**-0.57**
ΔP (RF)	**-0.70**	**-0.67**	**-0.71**	**-0.70**
T2 (CTR)	**0.27**	**0.31**	**0.37**	**0.44**
ΔT2 (CTR)	**-0.64**	**-0.65**	**-0.64**	**-0.64**
P (CTR)	**-0.32**	**-0.27**	(-0.23)	(-0.18)
ΔP (CTR)	**-0.76**	**-0.77**	**-0.74**	**-0.67**
T2 (Trc4)	**0.70**	**0.62**	**0.58**	**0.59**
T2 (Cook et al)	**0.20**	**0.24**	**0.31**	(0.34)

Table 2: Correlation indices with the NAO index. Considered time series are: the European surface air temperature T2, meridional temperature contrast ΔT2, precipitation P, meridional precipitation contrast of the RF simulation (line 1 to 4 respectively), same quantities but for the CTR simulation (lines 5 to 8), the European surface air temperature T2 of the Trc4 reconstruction (line 9) and of the Cook et al. (2002) reconstruction (line 10). Correlation considered the period 1550-1990 of the RF simulation and the second half of the CTR simulation. Brackets mark the values which are not significantly different from 0 at the 90% confidence level, while bold characters are used for significant values. The second to fifth columns consider the winter mean values (denoted as 1-winter) and the digitally low-pass filtered time series with a 10-year, 20-year, 40-year cut-off period, respectively.

Correlation with SVRF

	1-winter	10 y	20 y	40 y
T2 (RF)	**0.14**	**0.40**	**0.51**	**0.62**
T2 (Trc4)	**0.09**	**0.24**	(0.27)	(0.37)
NAO (RF)	(0.03)	(0.17)	(0.20)	(0.20)
NAO (Nrc2)	**0.12**	**0.26**	**0.32**	**0.43**
NAO (Cook)	(-0.02)	(-0.10)	(-0.18)	(-0.17)

Table 3: As for tab.2, but referring to the correlation with SVRF. First and second line: Average European temperature of RF simulation and of Trc4 reconstruction. Third to fifth line: NAO index of RF simulation, Nrc2 reconstruction and Cook et al. reconstruction.

Azores-Iceland SLP difference

	1000 y	450 y	125 y	70 y	25 y
CTR	20.9±0.4	20.8±0.6	21.6±1.2	21.7±1.4	22.6±2.5
RF		19.1±0.6	19.0±1.2	19.6±1.5	19.7±2.5
CRU			20.5±1.4	19.8±2.0	20.1±3.5

Table 4: Mean value and standard deviation (in hPa) of the winter sea level pressure difference between Azores and Iceland according to the CTR and RF simulations (first and second line), to the CRU (Climate Research Unit, East Anglia University dataset, third line). Values have been computed for the whole 1000 , and for the last 450, 125, 70 , 30 years of the datasets, when available.

Azores-Iceland SLP Variance

	1000 y	450 y	125 y	70 y	25 y
CTR	40<54<48	41<47<54	35<44<58	28<38<55	26<42<85
RF		44<49<57	40<50<66	30<40<59	24<39<78
CRU			53<67<88	52<70<102	50<81<162

Table 5: As for tab.4 but for the variance (in hPa^2). The lower and upper limit of the 95% confidence interval are also shown.

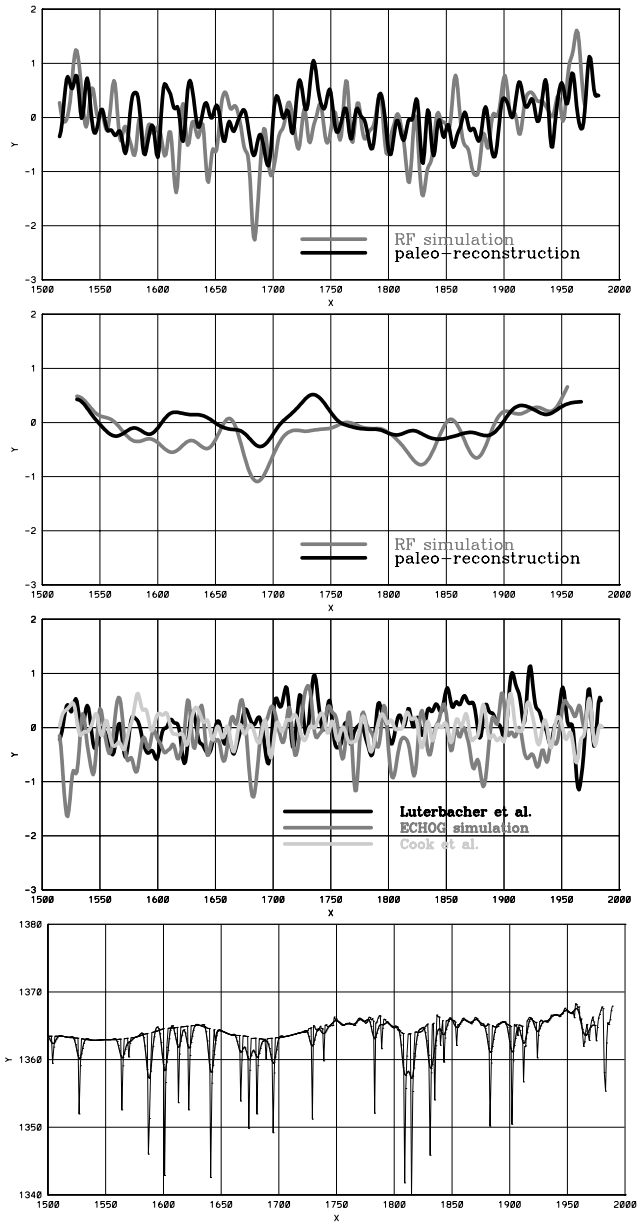

Figure 1: Top: Average European winter temperature over land since year 1500. Values are anomalies (in K) with respect to the average temperature in the 1850-1950 period. A low pass digital filter with a 10-year cut-off period has been applied to the data. The black curve shows the reconstruction Trc4 time series by Luterbacher et al. (2004). Second row: as the top panel, but filtered using a 40-year cut-off period. Third row: as the top panel but for the winter NAO index. The black line is the Nrc2 reconstruction by Luterbacher et al. (2002), the grey line shows the RF simulation, the pale grey curve shows the values of Cook et al. (2002). Bottom panel: total radiative forcing (in W/m^2) derived from reconstructions of net radiative forcing Crowley (2000) and rescaled to total solar irradiance. The thin line shows the winter mean values, the thick line shows the

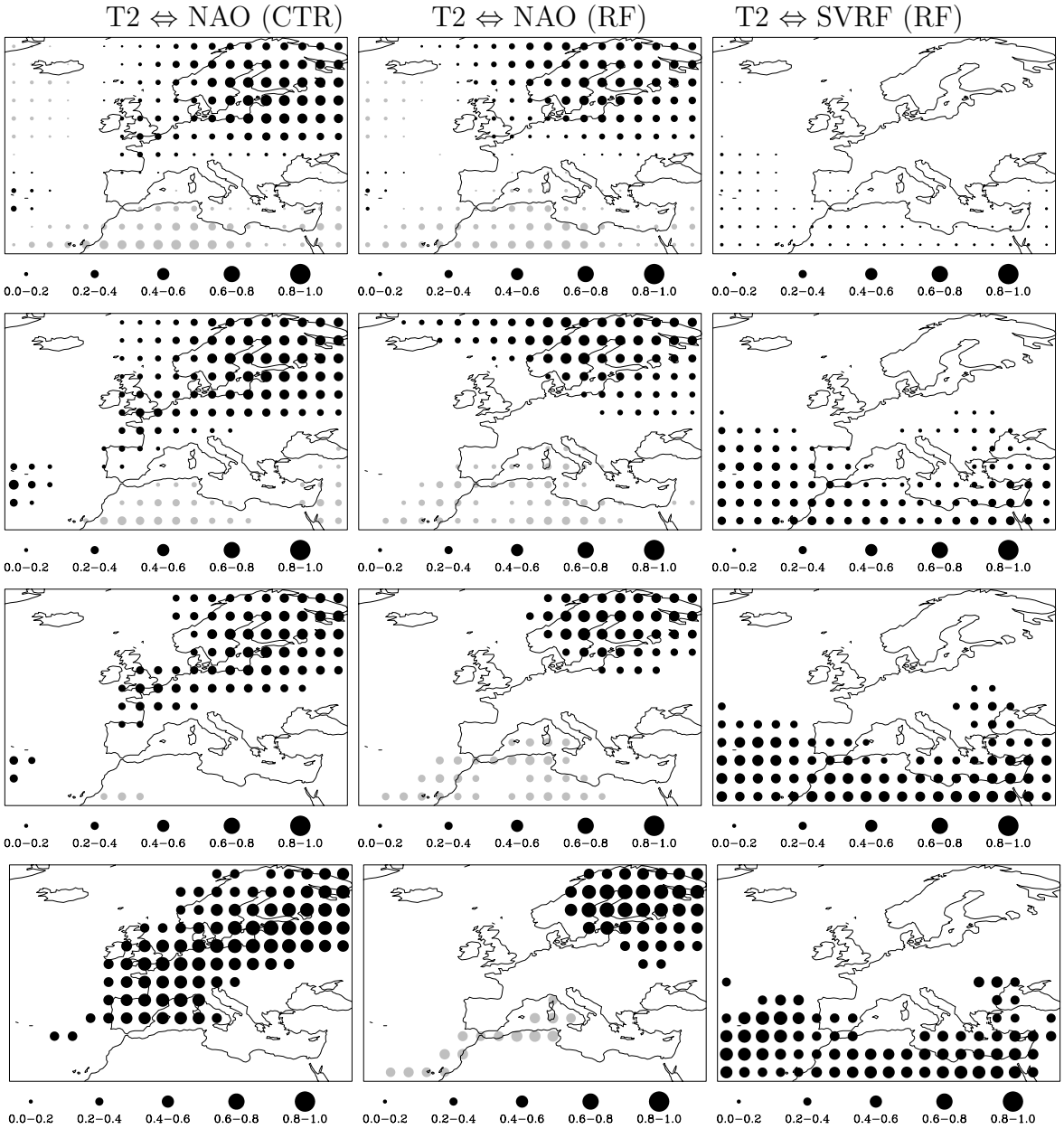

Figure 2: Spatial distribution of the correlation between the T2 and the NAO index in the CTR simulation (left column), in the RF simulation (central column), and between T2 and the SVRF in the RF simulation. The first row considers the winter mean values, second to fourth rows the digitally low-pass filtered data with a 10-year, 20-year, 40-year cut-off period, respectively. Black and grey dots denote positive and negative values, respectively. In the white areas the correlation is not significantly different from 0 at the 90% confidence level.

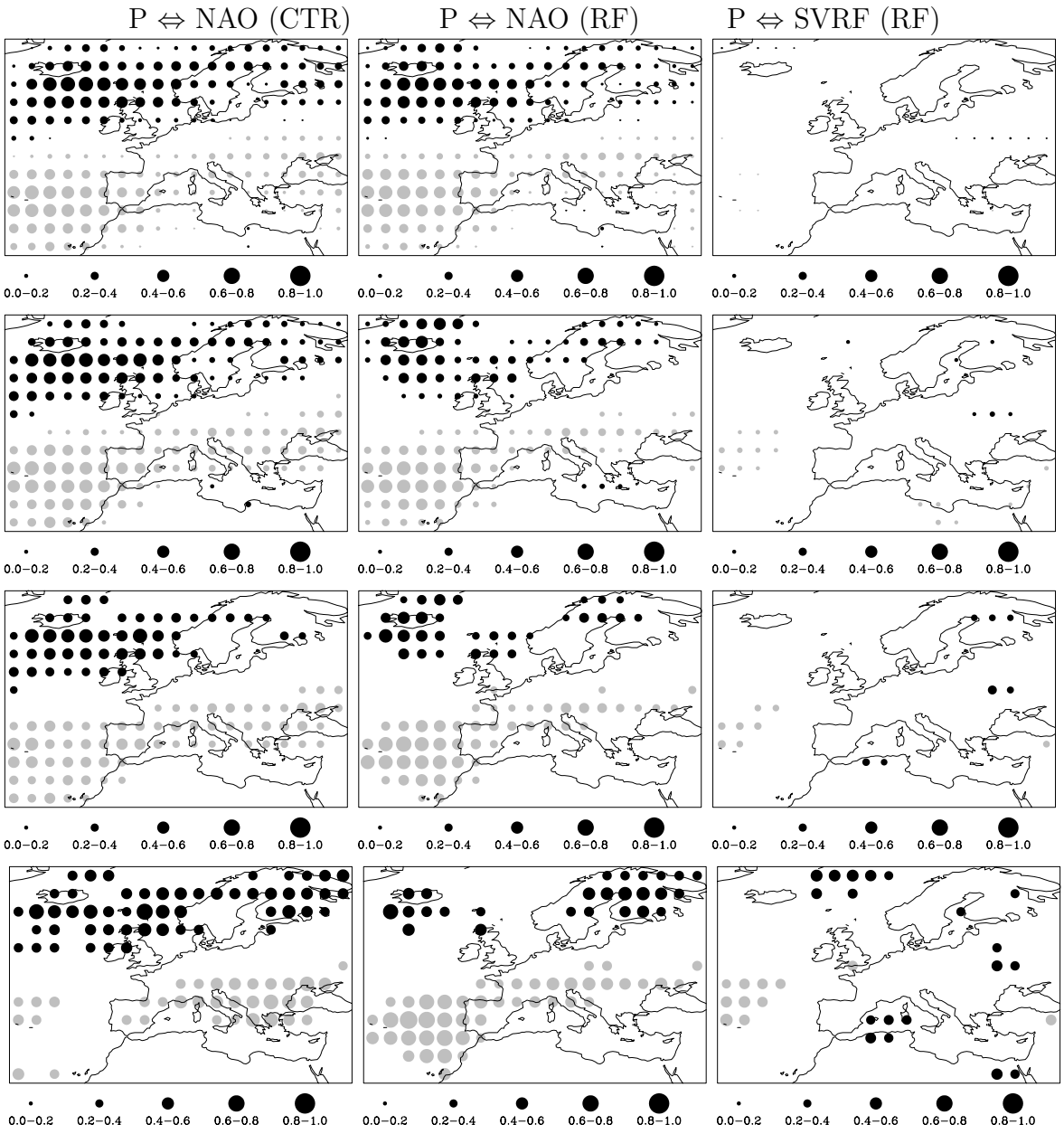

Figure 3: As for fig.3 , but for precipitation P.

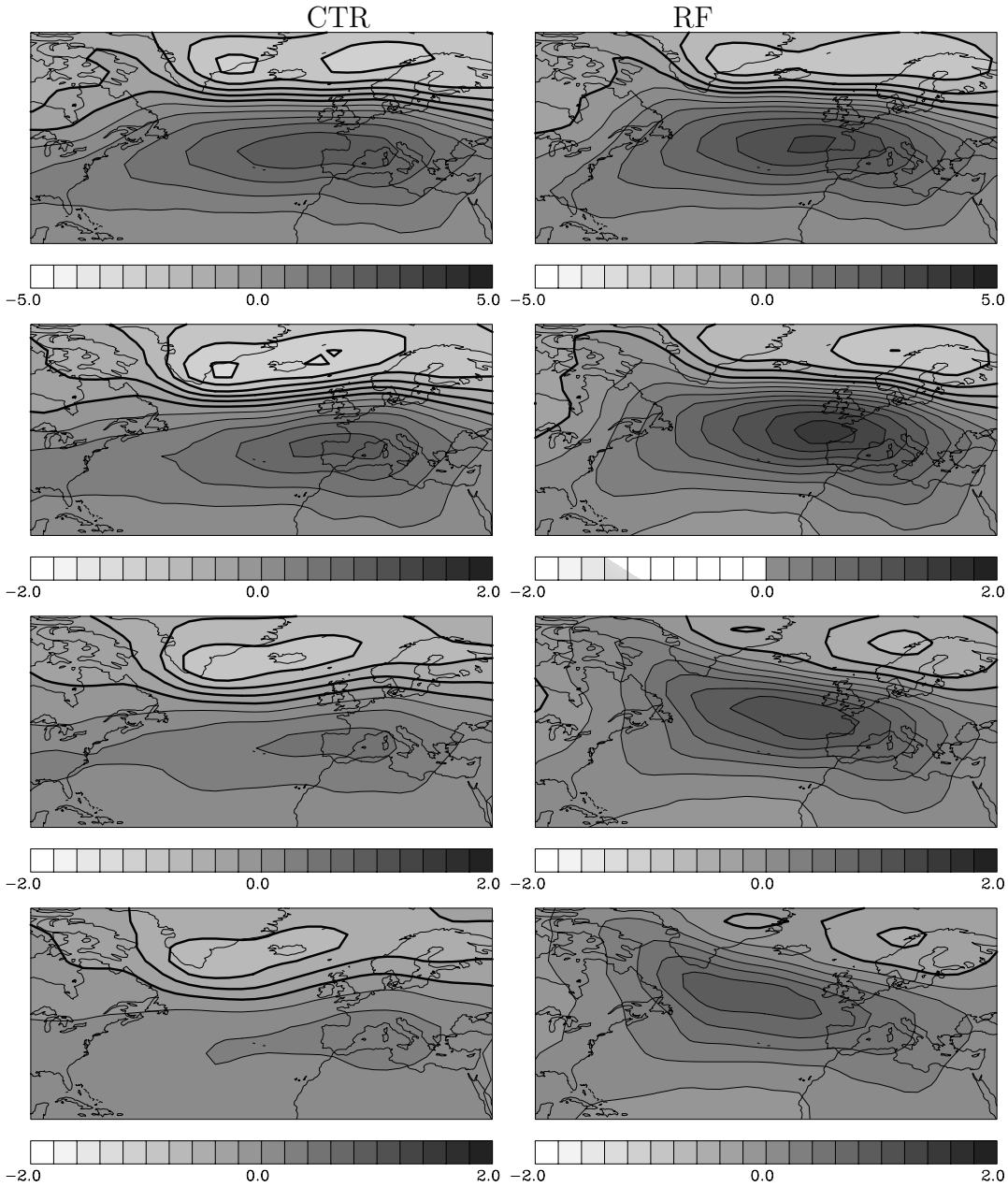

Figure 4: First EOF of the SLP fields for the CTR simulation (left column) and the RF simulation (right column). The first row shows the EOF resulting from the PCA of winter mean values, the second to fourth rows those resulting from the digitally low-pass filtered data with a 10-year, 20-year, 40-year cut-off period, respectively. The thick contour lines denote negative values.

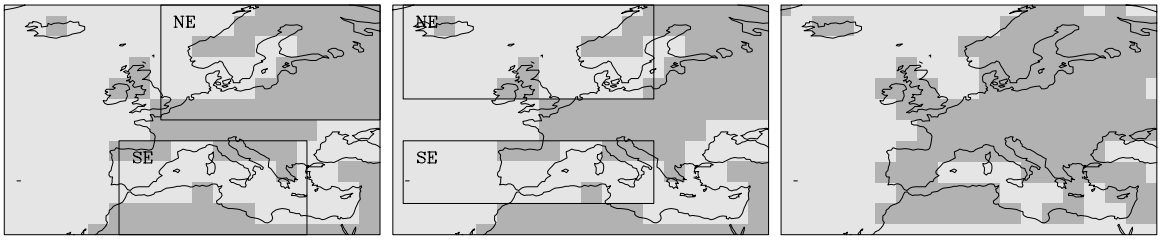

Figure 5: The land-sea mask of the ECHO-G simulations in the analysed area and the regions used for the computation of the North-South Europe contrast (left for T2, centre for P). Right panel: Land-sea mask of the Trc4 (Luterbacher et al, 2004) data up-scaled to the resolution of the ECHO-G simulations.

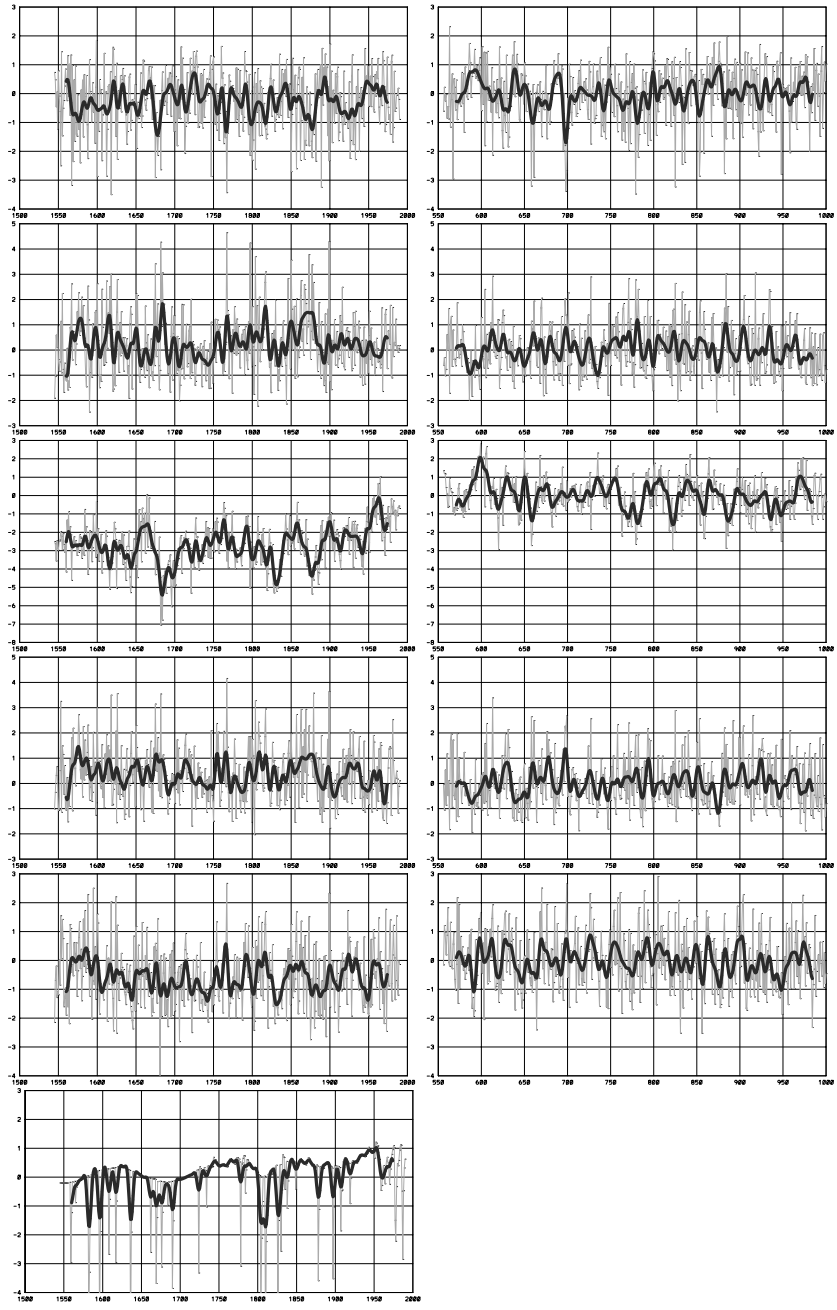

Figure 6: Indices of winter NAO (first row), North-South Europe temperature contrast (second row) , mean European Temperature (third row), North-South Europe precipitation contrast (fourth row), total precipitation over the European area (fifth row), radiative forcing (sixth row, left). Left panels refer to the RF simulation, right panels to the CTR simulation (last 450 years). The light lines show the actual winter mean values, the thick lines the low-pass filtered data with a 10 years cut-off periods. The indices are computed using the mean and the variance of the last 500 years of the CTR simulation.

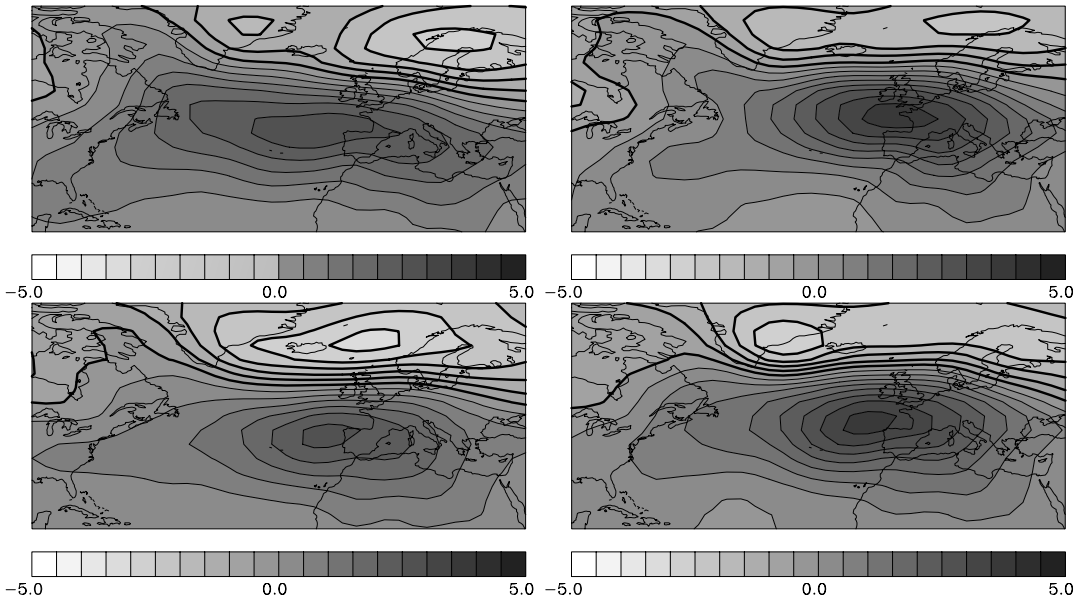

Figure 7: First EOF of the SLP field in the Atlantic for 4 different periods. RF simulation: 1660-1710 Maunder minimum (top left) and 1800-1840 Dalton minimum (top right). CTR simulation: 650-700 year (bottom left) and 400-450 (bottom right). The thick contour lines denote negative values.

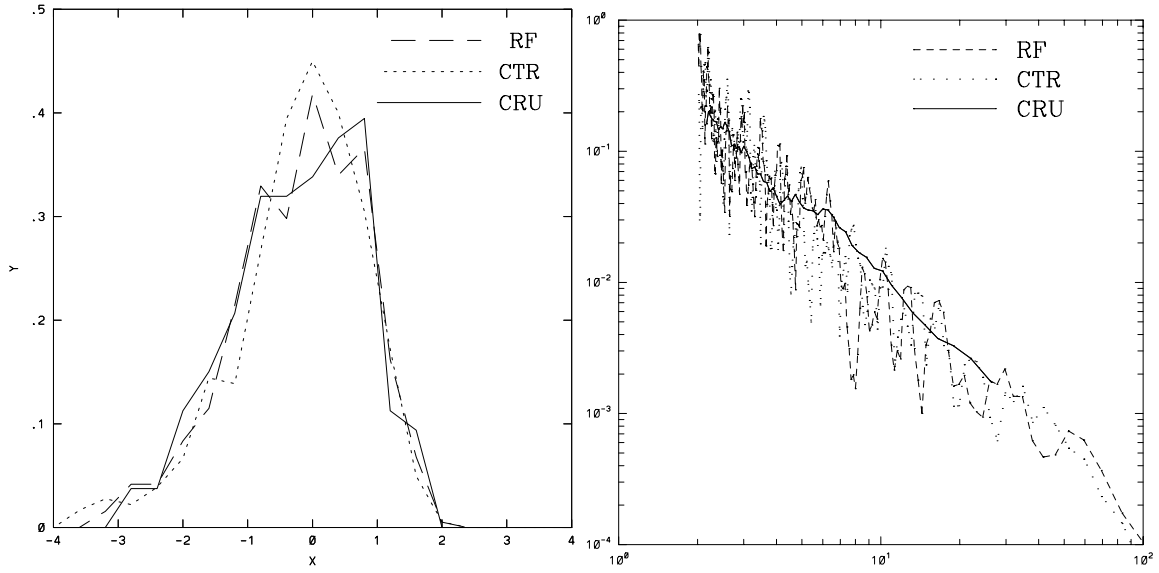

Figure 8: Left panel: distribution of the NAO index (probability, y-axis, as function of the index value (x-axis). Right panel: power spectra of the NAO index as function of period (in years). The curves refer to the CRU (continuous curve), RF (dashed curve), CTR (dotted curve) datasets.

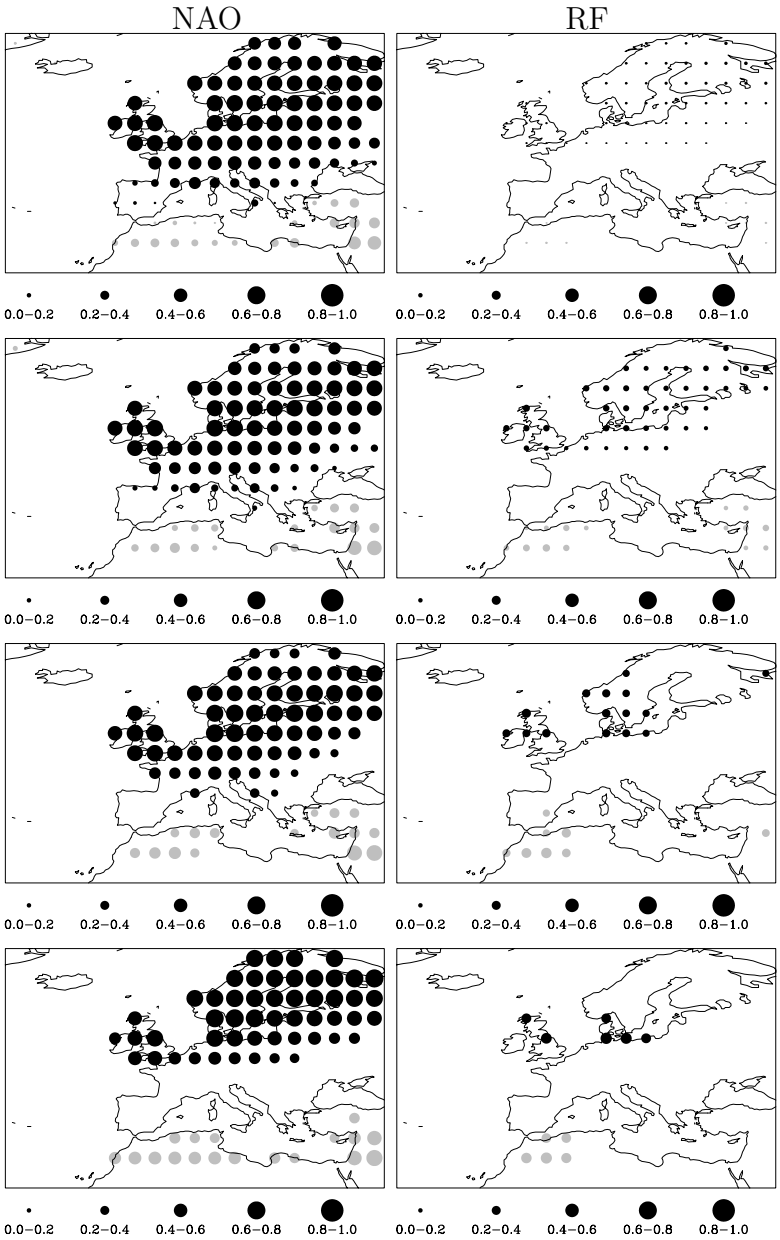

Figure 9: Reconstruction: correlation of the surface temperature fields with the NAO index (left column) and with the RF (right column). The first row considers the winter mean fields, second to fourth rows the digitally low-pass filtered fields with a 10-year, 20-year, 40-year cut-off period, respectively. Black and grey dots denote positive and negative values, respectively. In the white areas the correlation is not significantly different from 0 at the 90% confidence level.

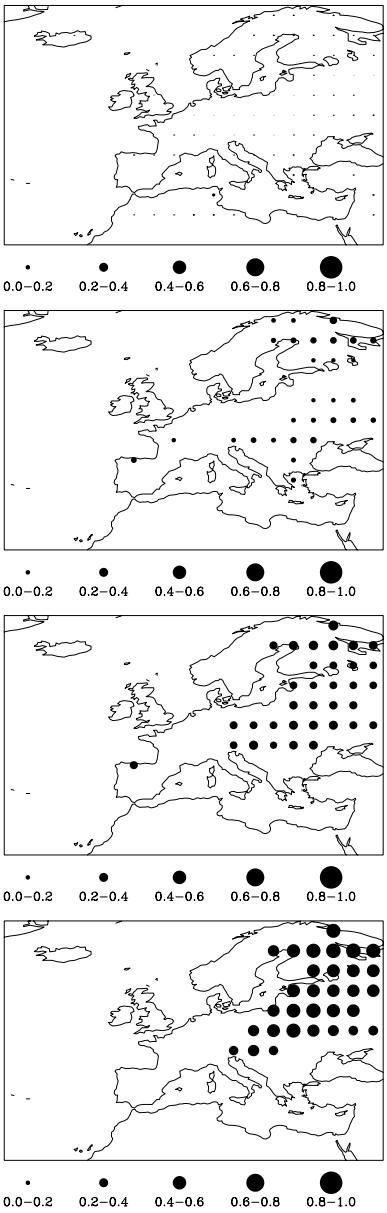

Figure 10: Correlation between the surface temperature fields of the reconstruction and the RF simulation. The first row considers the winter mean values, second to fourth rows the digitally low-pass filtered data with a 10-year, 20-year, 40-year cut-off period, respectively. Black and grey dots denote positive and negative values, respectively. In the white areas the correlation is not significantly different from 0 at the 90% confidence level.